J. Membrane Biol. 125, 107–118 (1992)

The Journal of
Membrane Biology

Spatial and Temporal Patterns of Intracellular Calcium in Colonic Smooth Muscle

Emeran A. Mayer, Anatoly Kodner, Xiao Ping Sun, Jonathan Wilkes, David Scott, and George Sachs
Center for Ulcer Research and Education, Departments of Medicine, VA Wadsworth Medical Center and University of California at Los Angeles, Los Angeles, California 90073; and Department of Physiology, University of California at Los Angeles, Los Angeles, California 90024

Summary. Intracellular calcium $[Ca^{2+}]_i$ measurements in cell suspension of gastrointestinal myocytes have suggested a single $[Ca^{2+}]_i$ transient followed by a steady-state increase as the characteristic $[Ca^{2+}]_i$ response of these cells. In the present study, we used digital video imaging techniques in freshly dispersed myocytes from the rabbit colon, to characterize the spatiotemporal pattern of the $[Ca^{2+}]_i$ signal in single cells. The distribution of $[Ca^{2+}]_i$ in resting and stimulated cells was nonhomogeneous, with gradients of high $[Ca^{2+}]_i$ present in the subplasmalemmal space and in one cell pole. $[Ca^{2+}]_i$ gradients within these regions were not constant but showed temporal changes in the form of $[Ca^{2+}]_i$ oscillations and spatial changes in the form of $[Ca^{2+}]_i$ waves. $[Ca^{2+}]_i$ oscillations in unstimulated cells ($n = 60$) were independent of extracellular $[Ca^{2+}]$ and had a mean frequency of 12.6 ± 1.1 oscillations per min. The baseline $[Ca^{2+}]_i$ was 171 ± 13 nM and the mean oscillation amplitude was 194 ± 12 nM. Generation of $[Ca^{2+}]_i$ waves was also independent of influx of extracellular Ca^{2+}. $[Ca^{2+}]_i$ waves originated in one cell pole and were visualized as propagation mostly along the subplasmalemmal space or occasionally throughout the cytoplasm. The mean velocity was 23 ± 3 μm per sec ($n = 6$). Increases of $[Ca^{2+}]_i$ induced by different agonists were encoded into changes of baseline $[Ca^{2+}]_i$ and the amplitude of oscillations, but not into their frequency. The observed spatiotemporal pattern of $[Ca^{2+}]_i$ regulation may be the underlying mechanism for slow wave generation and propagation in this tissue. These findings are consistent with a $[Ca^{2+}]_i$ regulation whereby cell regulators modulate the spatiotemporal pattern of intracellularly generated $[Ca^{2+}]_i$ oscillations.

Key Words Ca^{2+} oscillations · Ca^{2+} wave · sarcoplasmic reticulum

Introduction

Changes in $[Ca^{2+}]_i$ mediate a large variety of cellular responses, such as contraction, secretion and cell growth. The characteristic response seen in suspensions of smooth muscle cells is a $[Ca^{2+}]_i$ transient followed by an elevated steady-state increase (Bitar et al., 1986; Takuwa, Takuwa & Rasmussen, 1990). In contrast, single-cell fluorescence recording has shown that receptor-mediated Ca^{2+} signalling can be oscillatory in nature, allowing for frequency as well as amplitude modulation of the response (Orchard, Eisner & Allen, 1983; Woods, Cuthbertson & Cobbold, 1986; Ambler et al., 1988; Berridge & Galione, 1988; Gray, 1990; Jacob et al., 1988; Cobbold, 1989). Single-cell imaging studies have also shown that in various cell types, different spatial patterns of the $[Ca^{2+}]_i$ response can be detected (Berridge, 1988; Cheek, 1989; O'Sullivan et al., 1989; Rooney, Sass & Thomas, 1990). A combination of amplitude, frequency and spatial responses of receptor-mediated $[Ca^{2+}]_i$ changes could allow a cell to respond differentially to Ca^{2+}-mobilizing agonists. Reported spatio-temporal patterns include differences in the spatial $[Ca^{2+}]_i$ distribution between agonists in chromaffin cells (Cheek, 1989), oscillations with agonist-induced frequency and amplitude modulation in a variety of excitable and non-excitable cells (Berridge & Galione, 1988; Cobbold, 1989; Gray, 1990) and propagation of $[Ca^{2+}]_i$ gradients (Berridge, 1988; Berridge & Galione, 1988; Cornell-Bell et al., 1990; Takamatsu & Wier, 1990).

In the specific case of gastrointestinal smooth muscle, a variety of responses has been described suggesting that this cell type also responds to agonists with spatio-temporal signalling patterns. Single cell imaging has suggested spatial heterogeneity of $[Ca^{2+}]_i$, with subplasmalemmal and nuclear $[Ca^{2+}]_i$ gradients (Williams et al., 1985; Williams, Becker & Fay, 1987). In homogeneous $[Ca^{2+}]_i$ distribution has been confirmed by electron microscopy and by electron probe analysis, which demonstrated central and peripheral compartments of sarcoplasmic reticulum (SR) (Devine, Somlyo & Somlyo, 1972; Bond et al., 1984; Kowarski et al., 1985). The presence of a temporal signalling pattern in the form of $[Ca^{2+}]_i$ oscillations is suggested by the presence of spontaneous (Benham & Bolton, 1986) or agonist-induced cyclical activity of Ca^{2+}-activated K^+ channels

(Mayer et al., 1989). Such periodic changes could play a role in slow wave generation since spontaneous membrane depolarization may be dependent on Ca^{2+} influx (Himpens & Somlyo, 1988; Langton, Burke & Sanders, 1989).

In this study using single-cell imaging techniques in colonic myocytes distinct spatio-temporal patterns of intracellular Ca^{2+} signalling are demonstrated. It is shown that (i) there is a distinct nonhomogeneous spatial distribution of $[Ca^{2+}]_i$; (ii) $[Ca^{2+}]_i$ changes in an oscillatory fashion; (iii) $[Ca^{2+}]_i$ gradients originating from one cell pole can spread along the longitudinal axis; and (iv) different stimuli result in distinct $[Ca^{2+}]_i$ responses.

Materials and Methods

Preparation of Single Myocytes

Myocytes were dispersed from the longitudinal muscle layer of the distal rabbit colon as previously described (Mayer et al., 1989). A 5-cm long piece of colon was removed, rinsed and placed in ice-cold physiological salt solution (PSS)-A (in mM): 126.0 Na^+, 6.0 K^+, 1.0 Ca^{2+}, 1.2 Mg^{2+}, 132 Cl^-, 11 glucose, 10 N-2-hydroxyethylpiperazine-N'-2-ethanesulfonic acid (HEPES), titrated with NaOH to pH 7.4. Pieces of the longitudinal muscle layer were removed under a dissecting microscope and incubated in the dispersion solution in a shaking bath at 37°C. The dispersion solution (20 ml) was PSS-A containing 10 mg type 2 collagenase (Cooper Biomedical), 20 mg trypsin inhibitor (Sigma) and 50 mg bovine serum albumin (BSA: Sigma). Following a 10-min incubation period, the tissue was removed, placed into PSS-A at room temperature and gently dispersed using a firepolished pasteur pipette. Imaging results obtained in cells dispersed in PSS-A, in which the $[Ca^{2+}]$ was lowered to 100 μM did not differ from those prepared in 1.0 mM Ca^{2+}.

Immediately following dispersion, aliquots of cells were incubated in PSS-B containing (in mM): 100 Na^+, 5.4 K^+, 1.2 Mg^{2+}, 1.0 Ca^{2+}, 109.8 Cl^-, 10 pyruvate, 10 aspartate, 10 fumarate, 10 glutamate, 20 HEPES, 2 mg/ml BSA 5 μM 1-(2-5'-carboxyoxazol-2'-*yl*)-6 aminobenzofuran-5-oxy-(2'-amino-5'-methylphenoxy) ethane-N,N,N',N'-tetraacetic acid acetomethoxy ester (fura-2/AM: Molecular Probes, Eugene, OR). Cells were incubated for 30 min at 37°C without agitation. Cells were then washed by centrifugation, resuspended in and incubated in PSS-B for at least 20 min to allow de-esterification of internalized fura-2/AM. A suspension of cells was kept at room temperature, and aliquots were removed for measurements. The viability of cells was confirmed by their contractile response to agonists. Visual evaluation of fura-2 fluorescence revealed diffusely fluorescent cells.

Image Analysis

Intracellular calcium levels in individual myocytes were estimated using fura-2 fluorescence monitored with an image analysis system (Jacob et al., 1988). Fura-2 loaded myocytes adhered to the bottom of a perfusion chamber (100 μl volume). PSS-A was continuously circulated through the chamber at a rate of 1 ml per min. To minimize the contractile response of cells to agonists, the bath fluid was kept at 25°C. The time period for complete exchange of the bath solution during superfusion was <15 sec. Cells were observed through a Nikon Fluo 40 objective with a Zeiss Axiomat microscope in the epifluorescence mode using a long pass filter cutoff at 510 nm. Alternating excitation wavelengths of 340 and 380 nm were provided by a 75 W Xenon lamp, filtered by interference filters mounted in a rotating filter wheel, via the epifluorescence port of the microscope. The imaged field was monitored by a COHU ISIT camera. Image pairs were generally captured at a sampling rate of two frames per sec under the control of TARDIS software, and stored as digitized 256 gray level images. Subsequent digital image analysis was performed under the control of TARDIS software using a Joyce-Loeble Magical Image Processor. Following subtraction of background autofluorescence, R_{max} and R_{min} were determined from image pairs of cells equilibrated with ionomycin (5 μM) and EGTA (10 mM). R_{max} and R_{min} are the maximum and minimum 340/380 nm ratios obtained at saturating or zero $[Ca^{2+}]$. These parameters were used by the image processor to relate the ratio of each 340, 380 nm pair to $[Ca^{2+}]$ using a K_D value of 224 nM (Ambler et al., 1988; Jacob et al., 1988). Autofluorescence of myocytes was determined following quenching of the signal in ionomycin treated cells with 2 mM manganese chloride (Grynkiewicz, Poenie & Tsien, 1985). Following this procedure, fluorescence could no longer be detected at either wavelength. Images were processed in pairwise fashion, and the final result was displayed on a video monitor screen in 32 shades of pseudo-color, with blue colors representing low $[Ca^{2+}]_i$ and red–magenta colors representing high $[Ca^{2+}]_i$. To determine regional changes in $[Ca^{2+}]_i$, fluorescence was monitored over time within regions of the cell defined by the interactive software. Each field of view contained 1–3 cells.

To determine if regional increases in $[Ca^{2+}]_i$ were propagated along the cell, fluorescence ratios were monitored within up to five equally sized regions of interest, drawn along the longitudinal cell axis. The velocity of propagation was estimated from the distance between two adjacent regions of interest divided by the phase shift in the oscillation peak between these two areas. For quantitation of $[Ca^{2+}]_i$ oscillations the following definitions were used. The amplitude of $[Ca^{2+}]_i$ oscillations was defined as the change in $[Ca^{2+}]_i$ from the trough to the peak of oscillations. The baseline $[Ca^{2+}]_i$ was defined as the line drawn through the trough values of oscillations. The frequency of $[Ca^{2+}]_i$ oscillations was defined as the number of full oscillations per min.

Electron Microscopy

Rabbits were anesthetized with nembutal (50 mg/kg). The aorta was canulated and the animal was perfused for 2 min with phosphate buffer containing 5 U/ml heparin. Following the initial perfusion, the perfusate was switched to a solution containing 4% paraformaldehyde and 3% glutaraldehyde (pH 7.4), and the perfusion continued for an additional 10 min. A piece of distal colon was then removed and placed in phosphate buffer. Strips of tissue 4 mm long and 1 mm wide were cut along the longitudinal axis of the longitudinal muscle layer for further tissue processing. Post fixation was completed in 2% OsO_4 for 1 hr following repeated washing of tissue strips in phosphate buffer. Tissues were dehydrated in graded steps of ethanol to a final concentration of 100%. Tissue strips were infiltrated in 50/50 100% ethanol and Polybed resin (Polysciences) for 2 hr, followed by overnight incubation in 100% resin. Embedding was completed in uncapped Beem capsules and polymerized at 60°C overnight. 1 μm thick

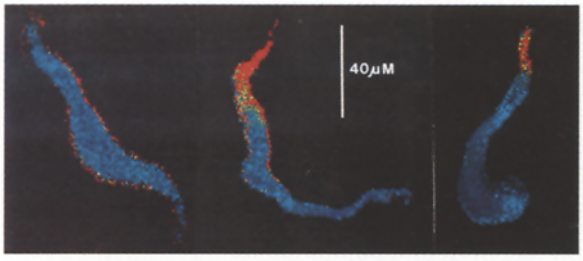

Fig. 1. Spatial distribution and temporal variations in $[Ca^{2+}]_i$ in unstimulated myocytes. Marked heterogeneity in cell length and distribution of $[Ca^{2+}]_i$ was noted. *Left panel* shows a representative cell in which a band of increased $[Ca^{2+}]$ is limited to the subplasmalemmal space. *Middle panel* shows a cell with partial contraction limited to the upper pole of the cell. Increased levels of $[Ca^{2+}]_i$ are seen within the cytoplasm of the contracted pole, whereas more distally they are progressively confined to the subplasmalemmal space. *Right panel* shows a regionally contracted cell (lower pole), in which the pole with increased cytosolic $[Ca^{2+}]$ does not correlate with the contracted pole. In this and subsequent figures the $[Ca^{2+}]_i$ concentration is displayed in pseudocolor images, with blue colors representing low $[Ca^{2+}]_i$, and red-magenta colors representing high $[Ca^{2+}]_i$. The background surrounding cells is displayed in black.

sections were cut for block orientation and stained with Toludine blue. 80 nm sections were cut with a diamond knife on a Reichert ultramicrotome and counterstained with uranylacetate (2%) and lead citrate, and examined in a Zeiss EM109 electron microscope.

Drugs and Chemicals

In addition to the chemicals mentioned above, the following compounds were used: carbamylcholine chloride (carbachol), caffeine, nifedipine, lanthanum trichloride ($LaCl_3$) (all Sigma). The synthetic NK-1 agonist [Sar^9,$Met(O_2)^{11}$]-SP was a generous gift from Dr. M. Regoli, University of Sherbrooke, Quebec.

Results

Cell Morphology

Dispersed myocytes varied considerably in their shape. Cells measured between 100 and 140 μm in length with a mean cell length of 125 ± 12 μm (n = 80). More than 50% of cells showed partial contractions limited to one cell pole (Fig. 1, middle and right panel), as defined by a widening of the cell diameter and/or a change from the characteristic cell tapering into a more rounded appearance of the cell pole. Less than 5% of cells were fully contracted and were not used for image analysis.

Electron microscopy of the cells showed characteristic features of intracellular structures. As shown in Fig. 2, in longitudinal sections through the plane of the nucleus, it was possible to visualize sarcoplasmic reticulum frequently with bound ribosomes both in the two conical regions near the poles of the nucleus, and close to the plasma membrane. In contrast, tubular structures were rarely seen in the rest of the cytoplasm. In the supranuclear regions, the tubular structures were located in the same region as the bulk of the mitochondria. In the subplasmalemmal space, tubules were frequently seen in association with caveolae. Supranuclear SR-like structures were most frequently seen limited to one cell pole, even though cells with a symmetrical distribution were also observed.

Spatial Distribution of $[Ca^{2+}]_i$

Regardless of cell geometry, the great majority of myocytes showed a characteristic, nonhomogeneous distribution of Ca^{2+} in the cytosol. This pattern was constant over time and not related to cell movements. Two patterns were observed. In one (70% of cells) there was a narrow band of elevated Ca^{2+} confined to the subplasmalemmal regions whereas the rest of the cytoplasma showed homogeneous, low levels of $[Ca^{2+}]_i$ (Fig. 1, left panel). In the other (25% of cells), and additional region of high $[Ca^{2+}]$ was seen throughout the cytoplasm in the supranuclear space of one cell pole (Fig. 1, middle and right panel). Thus, $[Ca^{2+}]_i$ gradients were not confined to edges and ends of cells, areas which may be susceptible to sampling artifacts. In the second group of cells, three regions of $[Ca^{2+}]_i$ could be distinguished along the length of the cell. The supranuclear region with elevated $[Ca^{2+}]_i$ occupied 26 ± 3% (range 10–50%) of the total cell length. In the adjacent segment, the elevated $[Ca^{2+}]_i$ was progressively confined to the subplasmalemmal region, and towards the opposite pole only the subplasmalemmal region showed $[Ca^{2+}]_i$ elevations as in the first pattern described. Regardless of cytosolic distribution, $[Ca^{2+}]_i$ was always highest in the subplasmalemmal space. Nuclear or perinuclear $[Ca^{2+}]_i$ gradients were absent from both $[Ca^{2+}]_i$ patterns. As illustrated in Fig. 1, the type of pattern observed did not correlate well with the overall cell length or the presence of regional contractions. Even though the contracted pole of a cell was more likely to contain zone 1 (Fig. 1, middle panel), the opposite, relaxed pole frequently showed the regional increase in cytoplasmic $[Ca^{2+}]$ (Fig. 1, right panel). In less than 5% of cells, high cytoplasmic $[Ca^{2+}]$ values were found throughout the cell. These cells were not used for further analysis.

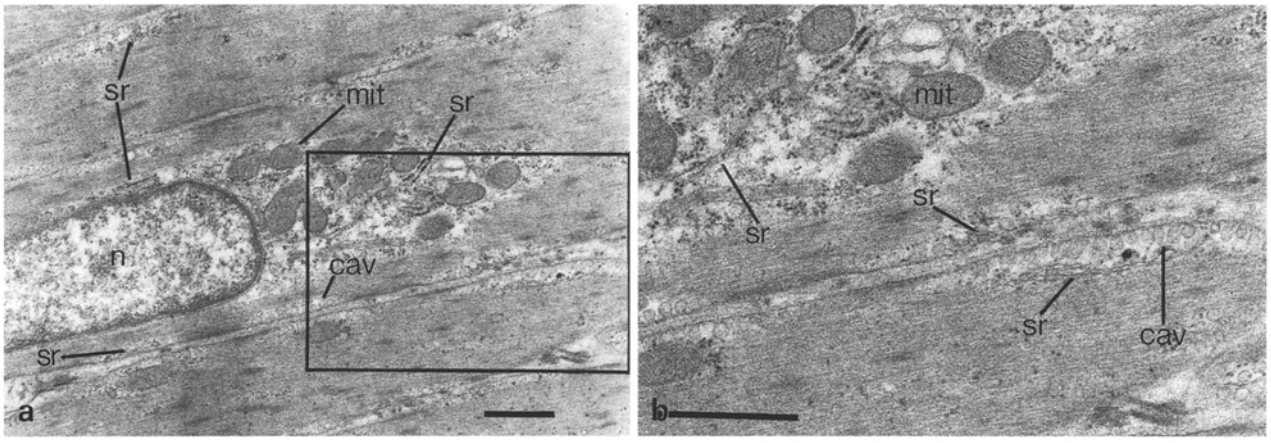

Fig. 2. Electron micrograph of myocyte from the longitudinal muscle layer of the distal rabbit colon in longitudinal section. Several myocytes, one displaying nucleus (*n*), are shown. *sr*, sarcoplasmic reticulum of both smooth and granular types; *mit*, mitochondria; *cav*, caveolae. Calibration bar, 1 μm.

Neither the dihydropyridine antagonist nifedipine, in concentrations that block L-type Ca^{2+} channels in this tissue (3×10^{-7} to 3×10^{-6} M) (Mayer et al., 1990) nor lanthanum (La^{3+}; $1–5 \times 10^{-5}$ M) affected the nonhomogeneous distribution of cell $[Ca^{2+}]$ visualized by fura-2. However, as shown in Fig. 3*a*, La^{3+} attenuated the amplitude of spontaneous subplasmalemmal $[Ca^{2+}]_i$ oscillations, and this effect was reversed by chelating La^{3+} with micromolar concentrations of EGTA (50 μM). As the affinity of EGTA for La^{3+} is several orders of magnitude greater than for Ca^{2+} (Martel & Smith, 1974), addition of 50 μM EGTA will completely chelate La^{3+} but leave the bath $[Ca^{2+}]$ virtually unaffected (0.95 mM). When cells were perfused with a 126-mM KCl solution in which the free $[Ca^{2+}]$ was buffered to 5×10^{-8} M, spontaneous Ca^{2+} oscillations were greatly attenuated (Fig. 3*b*).

The nonhomogeneous pattern of $[Ca^{2+}]_i$ was also found in stimulated cells, but was not related to cell movement. Depolarization with 126 mM KCl perfusate (containing 1 mM Ca^{2+}) which increases voltage-sensitive Ca^{2+} influx resulted in a transient increase in $[Ca^{2+}]_i$ of variable duration. This increase was evident in the supranuclear region and the subplasmalemmal space (Fig. 4). The region of $[Ca^{2+}]_i$ increase thus reflected the distribution of fura-2 fluorescence previously observed in unstimulated cells. As shown in Fig. 5, stimulation by caffeine also reflected the $[Ca^{2+}]_i$ pattern described here. In five out of six cells, caffeine resulted in an elevation of the subplasmalemmal $[Ca^{2+}]$, and where a polar distribution was observed, the most pronounced increase in fluorescence occurred at the polar region. The response to superfusion with carbachol ($10^{-6}–10^{-4}$ M) was studied in 12 cells. In the nine cells responding with an increase in $[Ca^{2+}]_i$ two spatial patterns were observed. In three cells, the changes in $[Ca^{2+}]_i$ were distributed as in the resting cell, being seen in one pole and in the subplasmalemmal space. In three cells a transient crescent-shaped $[Ca^{2+}]_i$ change along one side of the cell extending 20–30% towards the midline was seen prior to the increase in the polar region (Fig. 6*a*). The associated changes in $[Ca^{2+}]_i$ occurred so rapidly, that it was only reflected in one data point (upper part of Fig. 6*a*). Given the sampling rate of one image pair per second, reliable imaging of this event was therefore not possible. The possibility of a sampling artifact causing the initial rapid response, however, is unlikely since immediate $[Ca^{2+}]_i$ changes were only seen in response to carbachol but not to any other stimulus tested.

Three physiological explanations have been advanced to explain the nonhomogeneous distribution of fura-2 fluorescence in similar cell types (Williams et al., 1985; Alkon & Rasmussen, 1988; Somlyo & Himpens, 1990). One suggestion is that fura-2 fluorescence reports on Ca^{2+} levels within the SR (Williams et al., 1985). However, it has been shown that fura-2 does not penetrate the SR and further that the SR does not contain esterases capable of liberating fura-2 from fura-2 AM (Somlyo & Himpens, 1990). In the current experiments, agents known to release Ca^{2+} from the SR, such as caffeine, increased the fura-2 fluorescence rather than decreasing it, making this hypothesis unlikely. A second explanation invokes transmembraneous cycling of Ca^{2+} resulting from prolonged influx through voltage-sensitive Ca^{2+} channels and extrusion via the plasma membrane Ca^{2+} pump (Alkon & Rasmussen, 1988). Since neither nifedipine nor La^{3+} affected the distribution

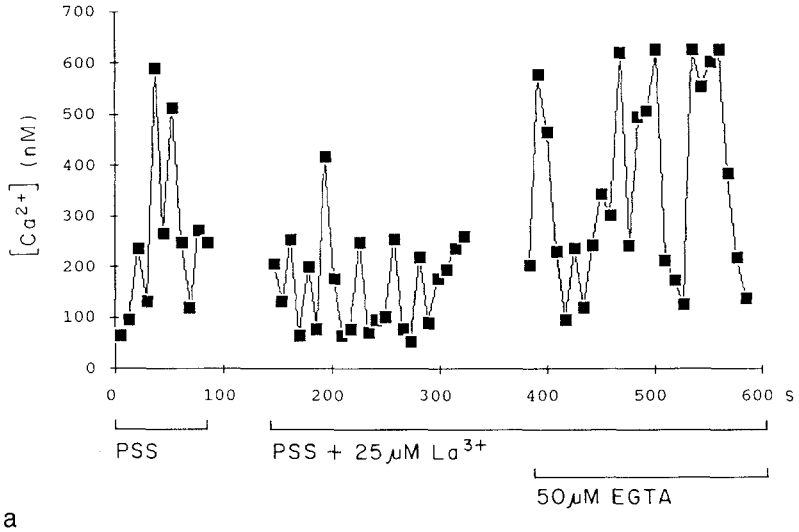

a

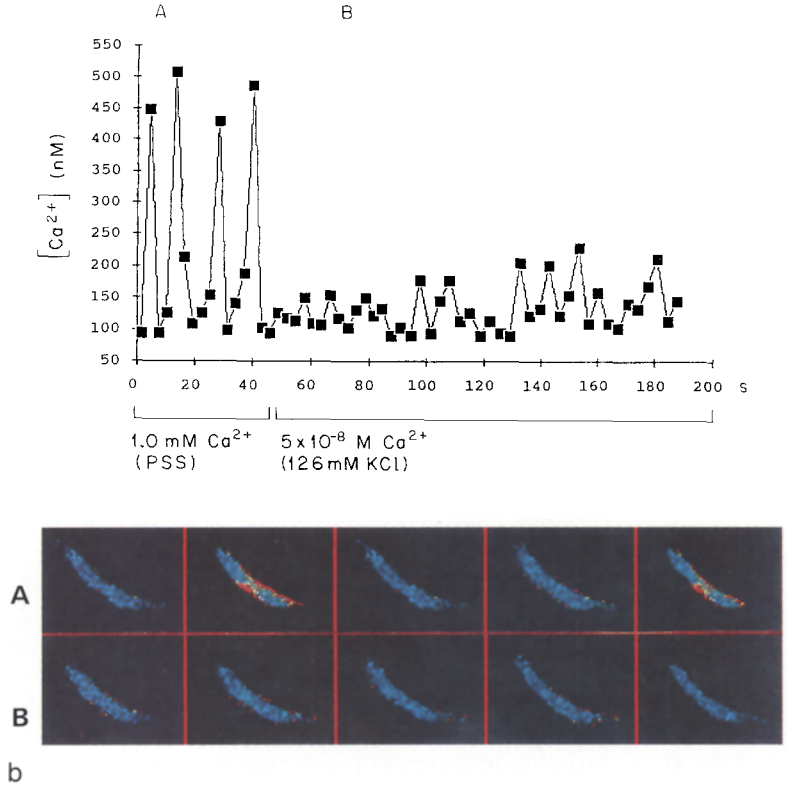

b

Fig. 3. Dependence of spontaneous $[Ca^{2+}]_i$ oscillations on influx of extracellular Ca^{2-}. (*a*) Effect of La^{3-} on spontaneous $[Ca^{2+}]_i$ oscillations. Representative experiment showing the partial inhibition of the amplitude of spontaneous $[Ca^{2-}]_i$ oscillations by 25 μM La^{3+}. No effect on frequency of oscillations was observed. The inhibitory effect was reversed instantaneously by chelation of La^{3+} with 50 μM EGTA. Based on the much higher affinity of EGTA for La^{3+} as compared to Ca^{2+} (Martel & Smith, 1974), the free $[Ca^{2-}]$ of the PSS solution in the presence of 50 μM EGTA remains almost unchanged at 0.95 mM. In this and subsequent figures, the bath temperature was 22°C. (*b*) Dependence of $[Ca^{2+}]_i$ oscillations on extracellular $[Ca^{2+}]$. *Upper part:* Representative experiment showing the prompt disappearance of spontaneous $[Ca^{2+}]_i$ oscillations following the exchange of the bath solution from PSS to 126 mM KCl solution containing 5×10^{-8} M Ca^{2+}. (*A* and *B*) above the trace refer to the color plates shown in the lower part of the Fig. *Lower part:* Shown are consecutive pseudocolor images of a myocyte when bathed in PSS (1 mM Ca^{2+}) (*A*, upper panel) and following the exchange of the bath solution to 126 mM KCl (5×10^{-8} M Ca^{2+}) (*B*, lower panel).

of $[Ca^{2+}]_i$, voltage-sensitive Ca^{2+} entry was not a requirement for the spatial heterogeneity of Ca^{2+}.

Nonhomogeneous $[Ca^{2+}]_i$ distributions could also arise from various sampling artifacts. For example, movement of cells between the capture of the 340 and 380 nm image either in the form of contraction or movement within the chamber could result in sampling artifacts at the cell edges. However, $[Ca^{2+}]_i$ gradients were not limited to the cell edges, and the continuous presence of these gradients would require a constant movement of the cell synchronous with the sampling rate. Similarly, ratioing of images with low signal-to-noise ratios could result in region with artifactual high $[Ca^{2+}]_i$. However, submembranous fluorescence gradients were also seen in the respective 340 and 380 nm images before ratioing.

Thus, even though a contribution of the discussed factors to our findings cannot be completely ruled out, the most likely explanation for the nonho-

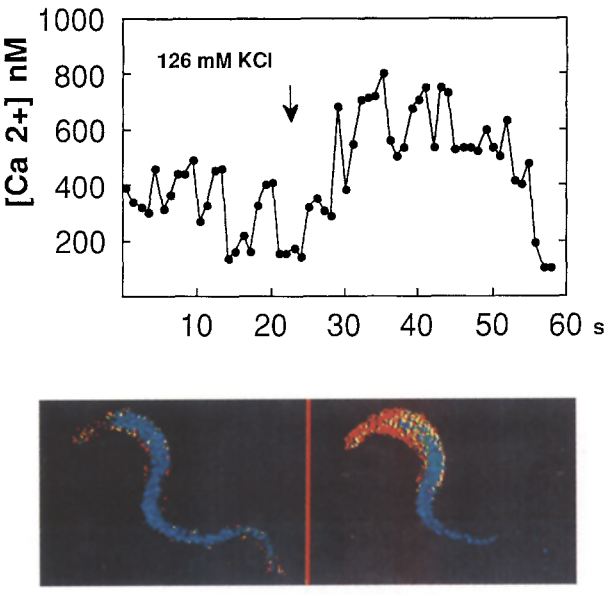

Fig. 4. The effect of membrane depolarization on the temporal and spatial pattern of $[Ca^{2+}]_i$. *Upper panel:* Representative experiment showing the increase of baseline $[Ca^{2+}]_i$ in response to membrane depolarization with 126 mM KCl solution. No effect on the amplitude of oscillations was observed. Experimental conditions were the same as described in Fig. 3. *Lower panel:* Individual pseudocolor images from the experiment shown above illustrating the spatial distribution of the $[Ca^{2+}]_i$ under control conditions (left) and following the exchange of the bath solution with 126 mM KCl solution (right). Display in pseudocolors is the same as described in Fig. 1 and Materials and Methods.

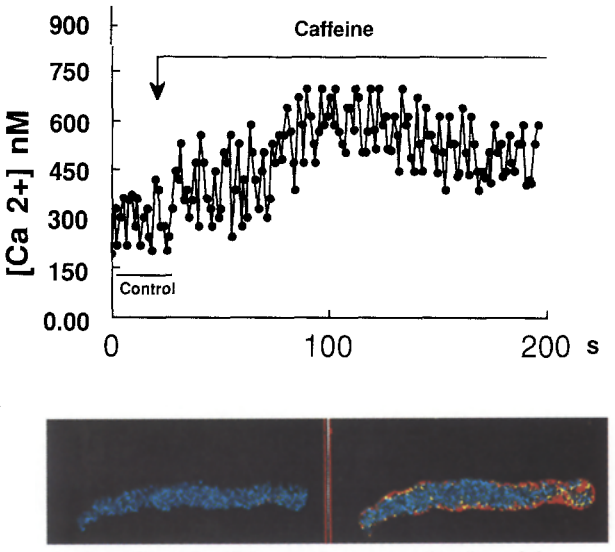

Fig. 5. The effect of caffeine on the temporal and spatial pattern of $[Ca^{2+}]_i$. *Upper panel:* Representative experiment showing the stimulatory effect of caffeine on baseline $[Ca^{2+}]_i$ and on the amplitude of spontaneous $[Ca^{2+}]_i$ oscillations. No effect on frequency of oscillations was observed. Cells were continuously perfused with PSS or PSS containing 20 mM caffeine. Whole cell images were acquired at the rate of one image pair per sec. *Lower panel:* Individual pseudocolor images from the experiment shown above illustrating the spatial distribution of $[Ca^{2+}]_i$ under control conditions (left) and following addition of caffeine (right). The caffeine-induced stimulation of $[Ca^{2+}]_i$ occurred primarily in the subplasmalemmal space.

mogeneous distribution of $[Ca^{2+}]_i$ involves a finite permeability of the SR present in the pole of the cell and the subplasmalemmal space, with Ca^{2+} efflux and reuptake occurring even in unstimulated cells (Somlyo & Himpens, 1990). Cell stimulation results in enhanced release from this pool, maintaining the geometry found in unstimulated cells.

Temporal Variation of $[Ca^{2+}]_i$

In a variety of excitable and nonexcitable cells, oscillations in $[Ca^{2+}]_i$ have been reported (Orchard et al., 1983; Schlegel et al., 1987; Berridge & Galione, 1988). These oscillations can be generated by intermittent influx of extracellular Ca^{2+} through the plasmamembrane (membrane oscillator) by intermittent release from intracellular stores (cytosolic oscillator), or by a combination of both mechanisms. When fura-2 fluorescence was monitored within defined intracellular regions, $[Ca^{2+}]_i$ oscillations were observed in myocytes under control conditions and during superfusion with agonists. The presence of oscillations was observed in cells dispersed in low Ca^{2+}-containing solutions and was independent of the total $[Ca^{2+}]_i$ of individual myocytes, indicating that $[Ca^{2+}]$ oscillations are not a result of Ca^{2+} overloading of the SR. $[Ca^{2+}]$ oscillations were greatly attenuated when cells were bathed in 126 mM KCl solution with a free $[Ca^{2+}]$ of 5×10^{-8} M (Fig. 3*b*). Conversely, in cells without spontaneous $[Ca^{2+}]$ variations, oscillations could be induced by cell activation with an agonist (*see* Fig. 7*b*). These findings indicate that temporal variations in $[Ca^{2+}]$ are not random variations in the fluorescence signal but represent physiological variations. However, given the sampling rate of one image pair per sec, and the large variation in apparent oscillation frequency, aliasing in many of the experiments is to be expected. Aliasing is suggested by the observed temporal variation in oscillation amplitude (Figs. 5–7) and by the imaging of some oscillation peaks by only one data point (Fig. 3*b*). In cells with polar distribution of $[Ca^{2+}]_i$ ($n = 16$), the peak value of $[Ca^{2+}]_i$ within the polar region was 976 ± 11 nM and the nadir was 356 ± 40 nM. In the adjacent subplasmalemmal space, the value oscillated between 488 ± 43 and 189 ± 10 nM, and at the opposite end of the cell the respective values were 160 ± 8 and 50 ± 4 nM. The averaged values obtained from the entire cell

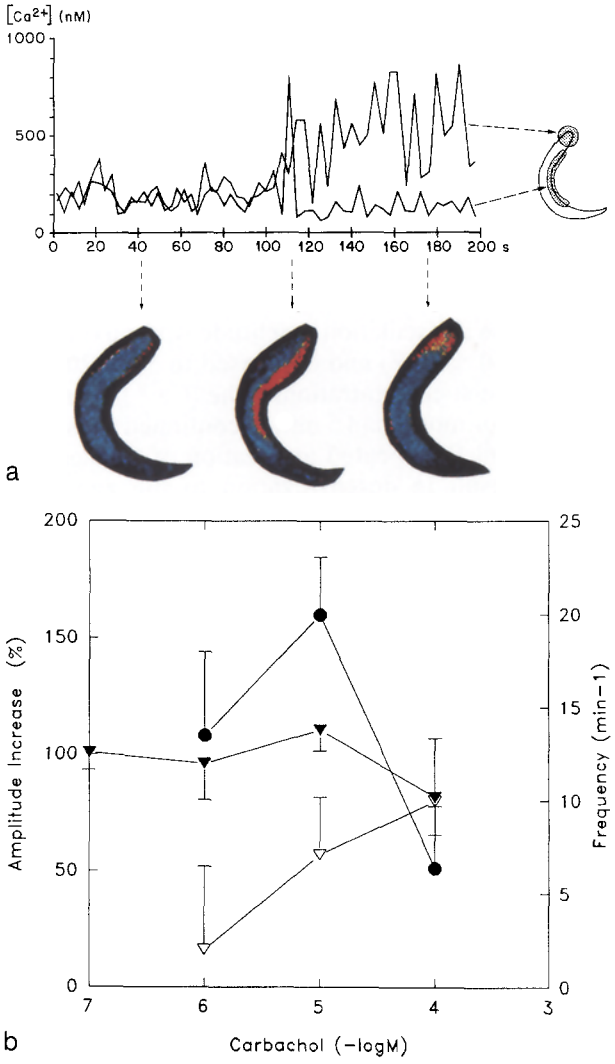

Fig. 6. Effect of carbachol on the temporal and spatial pattern of $[Ca^{2+}]_i$. (*a*) Representative experiment showing the time course of regional $[Ca^{2+}]_i$ changes in response to carbachol. The cartoon on the right of the graph shows the regions of interests in which fura-2 fluorescence was monitored. As indicated by the dotted arrows, the pseudocolor images underneath the graph illustrate representative $[Ca^{2+}]_i$ distribution patterns under control conditions (left), immediately following addition of carbachol (middle) and during the development of $[Ca^{2+}]_i$ oscillations in one cell pole. (*b*) Dose response relationship for global changes in baseline $[Ca^{2+}]_i$ (open triangles), oscillation amplitude (filled circles) and frequency of oscillations (filled triangles) obtained from experiments as shown in *a*. For the baseline and oscillation amplitude, mean values ± SE for the percent increase over prestimulation values are shown. Oscillation frequency is shown in number of oscillations per min. Each data point represents the mean from 4–10 experiments.

(n = 32) for the baseline $[Ca^{2+}]_i$ and the oscillation amplitude were 171 ± 12 and 194 ± 12 nM. The mean frequency of oscillations was 12.6 ± 1.1 per min (range 9–24.0). Oscillation frequency varied between individual cells despite constant

Table. Average parameters of agonist-induced $[Ca^{2-}]_i$ changes in individual myocytes

Condition	Cells	Baseline (nM)	Oscillations	
			Amplitude (nM)	Frequency
Control	60	171 ± 13	194 ± 12	12.6 ± 1.5
KCl (126 mM)	6	512 ± 45[a]	208 ± 18	13.8 ± 1.2
Caffeine (10 mM)	6	520 ± 51[a]	310 ± 28[a]	10.8 ± 1.5
Carbachol (10^{-5} M)	10	339 ± 25[a]	212 ± 15	11.3 ± 1.0
NK-1 (10^{-8} M)	10	232 ± 18	384 ± 23[a]	9.6 ± 1.0

Baseline $[Ca^{2+}]_i$, oscillation amplitude and frequency were determined as described in Materials and Methods. Shown are mean values ± SE.

[a] Significant difference to control values ($P < 0.05$).

sampling rates, consistent with a physiological variability.

Stimulation of the cell could in principle exert four types of effect: a tonic effect resulting in unchanged oscillations being superimposed on an elevated $[Ca^{2+}]_i$ (Gray, 1990); a change in the amplitude (Tsunoda, Stuenkel & Williams, 1990) or shape of oscillations (Woods, Cuthbertson & Cobbold, 1987); a change in the frequency of oscillations (Cobbold, 1989) or a combination of these.

We tested four agents, K^+ depolarization, caffeine, carbachol and a substance P analogue, all of which have been shown to stimulate $[Ca^{2+}]_i$ in intact smooth muscle preparations. All agents affected baseline $[Ca^{2+}]_i$, the amplitude of $[Ca^{2+}]_i$ or a combination of both, without affecting the frequency of oscillations.

Prolonged depolarization of the plasma membrane with 126 mM KCl solution containing 1.0 mM Ca^{2+} increased the baseline $[Ca^{2+}]_i$ by 214 ± 10% of control values without affecting the amplitude or frequency of $[Ca^{2+}]_i$ oscillations (n = 6) (Fig. 4 and the Table). Hence membrane depolarization resulted in a simple tonic effect on cytosolic $[Ca^{2+}]$. When the free $[Ca^{2+}]$ of the depolarizing solution was buffered to 5×10^{-8} M, $[Ca^{2+}]_i$ oscillations were greatly attenuated and the $[Ca^{2+}]_i$ decreased (Fig. 3*b*). The addition of the Ca^{2+} entry blocking agent La^{3+} (5×10^{-5} M) reduced the amplitude of spontaneous oscillations by 38 ± 3% without effect on their frequency (Fig. 3*a*) (n = 6).

As shown in Fig. 5 and the Table, activation of Ca^{2+} release from the SR by caffeine increased the amplitude of the oscillations by 104 ± 10% from control values, and the baseline $[Ca^{2+}]_i$ by 153 ± 11% (n = 6). There was no effect on oscillation frequency.

As shown in Fig. 7*a* and the Table, the NK-1

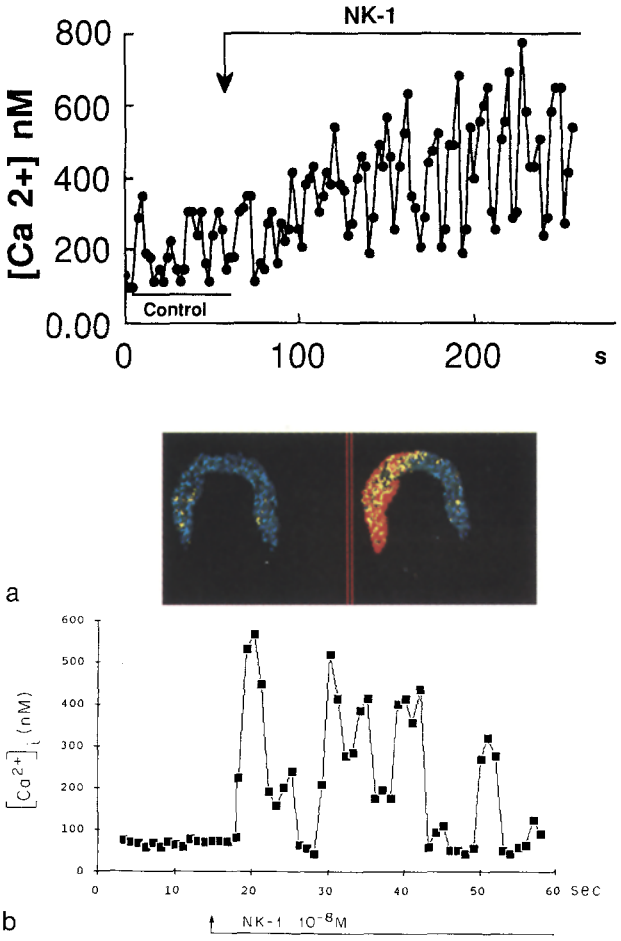

Fig. 7. Effect of the NK-1 agonist [Sar^9,Met(O$_2$)^{11}]-SP on the temporal and spatial pattern of $[Ca^{2+}]_i$. (*a*) *Upper panel:* Representative experiment showing the stimulatory effect of the NK-1 agonist on baseline $[Ca^{2+}]_i$ and on the amplitude of oscillations. No effect on the frequency of oscillations was observed. $[Ca^{2+}]_i$ represent average values from the whole cell. *Lower panel:* Individual pseudocolor images from the experiment shown above illustrating the spatial distribution of $[Ca^{2+}]_i$ under control conditions (left) and following exposure of the cell to the NK-1 agonist (10^{-8} M). (*b*) Representative experiment from a cell without detectable spontaneous $[Ca^{2+}]_i$ oscillations. Superfusion with the NK-1 agonist resulted in appearance of $[Ca^{2+}]_i$ oscillations. Fura-2 fluorescence was monitored from the supranuclear region of the cell.

agonist (10^{-10}–10^{-6} M) had a similar effect on baseline $[Ca^{2+}]_i$ and on the amplitude of $[Ca^{2+}]_i$ oscillations as caffeine, without affecting their frequency. For example, at a peptide concentration of 10^{-10} M, the observed increases in baseline and oscillation amplitude were 111 ± 5% and 36 ± 5%, respectively. In cells without spontaneous $[Ca^{2+}]_i$ oscillations, the peptide was able to induce oscillatory $[Ca^{2+}]_i$ changes (Fig. 7*b*). In the continued presence of the peptide, the increase in $[Ca^{2+}]_i$ persisted for up to several hundred seconds. However, repeated application of the peptide within 100 sec without prior superfusion of peptide-free solution resulted in a loss of the peptide's effect, suggesting desensitization.

Carbachol caused a pattern of $[Ca^{2+}]_i$ change similar to caffeine and the NK-1 agonist (Table). As shown in Fig. 6*b*, the relative effects on baseline $[Ca^{2+}]_i$ and oscillation amplitude were dose dependent. The baseline $[Ca^{2+}]_i$ concentration increased from 178 ± 15 nM at a dose of 10^{-6} M to 339 ± 25 nM at a dose of 10^{-4} M (n = 5–10). In contrast, the increase in oscillation amplitude was maximal at 10^{-6} M (160 ± 25%) and decreased to 51 ± 20% at higher agonist concentrations. The $[Ca^{2+}]_i$ increase persisted for more than 5 min in continued presence of the agonist. Repeated application of the agonist did not result in desensitization to the agonist's effect.

Spatio-Temporal Pattern

When $[Ca^{2+}]_i$ was monitored within subregions of cells, different spatio-temporal patterns were apparent. These patterns were observed in unstimulated cells and in cells activated by carbachol, NK-1 or membrane depolarization. In 80% of cells studied (n = 60), $[Ca^{2+}]_i$ peaks did not appear to occur simultaneously within different regions along the cell axis. Figure 8*a* shows five consecutive images of a cell following the application of carbachol (10^{-5} M). A region of increased $[Ca^{2+}]$ which is initially limited to the upper cell pole (first image) spreads throughout the cytoplasm to the nuclear region (images 2 to 4) before the sequence starts over again (last image). A propagation throughout the cytosol as illustrated by this experiment was observed in 5 out of 60 cells. Figure 8*b* shows a different cell during perfusion with the NK-1 agonists. In this cell a progressive phase shift of the $[Ca^{2+}]_i$ peak could be monitored through four different regions along the cell axis, consistent with a propagation of the $[Ca^{2+}]_i$ gradient. In contrast to the cell depicted in Fig. 8*a*, the propagation of the $[Ca^{2+}]_i$ signal appeared to be confined to the subplasmalemmal space. The mean speed of propagation calculated from the phase shift of the $[Ca^{2+}]_i$ peaks in nine cells was 23 ± 3 μm per sec (range 9 to 38 μm). Within a given cell, the speed calculated for regions at varying distances from the origin of propagation were similar without evidence for a proximal-to-distal gradient. Even though propagation was observed in unstimulated and cells activated by receptor occupation or membrane depolarization, $[Ca^{2+}]_i$ propagation was always from the pole with high $[Ca^{2+}]_i$ to the opposite pole. In the majority of cells, a phase shift in $[Ca^{2+}]_i$ peak between different regions of the cell was observed,

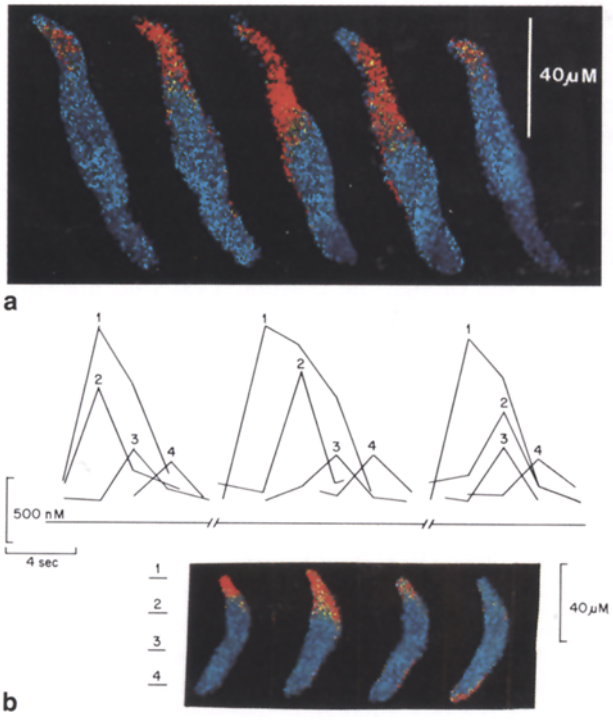

Fig. 8. Temporo-spatial pattern of $[Ca^{2+}]_i$. (*a*) Consecutive pseudocolor images from a myocyte following the application of carbachol (10^{-5} M). The experiment illustrates the spread of a region of high $[Ca^{2+}]_i$ arising in the upper pole of the cell (first image) to the center of the cell (images 2–4). This is followed by a return of the $[Ca^{2+}]_i$ distribution to the original pattern (last image). The apparent spread of the $[Ca^{2+}]_i$ gradient was observed throughout the cytoplasm. The cell length decreased by 10%. Images were captured at a rate of 2 per sec. (*b*) Representative experiment from a different myocyte following the application of the NK-1 agonist. Lower panel shows consecutive pseudocolor images of the cell, with apparent propagation of the area showing high $[Ca^{2+}]_i$ from one pole of the cell along the subplasmalemmal space to the opposite pole. Upper panel shows time course of $[Ca^{2+}]_i$ calculated from four different cell regions (*1–4*). Cell regions correspond to regions along the cell indicated to the left of pseudocolor panel. In three consecutive images, a phase shift in the oscillation peaks between the four monitored cell regions was observed. The speed of propagation was 32 μm per sec and was similar between different regions.

even though a continuous progression of a $[Ca^{2+}]_i$ wave through more than two cell regions could not be determined. In 20% of cells studied, the majority of peaks of $[Ca^{2+}]_i$ oscillations appeared to occur simultaneously.

Discussion

This study has shown that myocytes from the longitudinal muscle layer of the rabbit colon have a remarkably regulated spatio-temporal pattern of $[Ca^{2+}]_i$ signalling. The data presented demonstrate (i) the presence of spatially distinct intracellular Ca^{2+} pools, (ii) $[Ca^{2+}]_i$ oscillations, and (ii) propagation of $[Ca^{2+}]_i$ changes from one cell pole along the longitudinal cell axis.

Our data are consistent with the assumption that the subplasmalemmal $[Ca^{2+}]_i$ gradients observed in the majority of myocytes reflect increased levels of free cytosolic Ca^{2+} in the immediate vicinity of peripheral and central SR (Devine et al., 1972; Bond et al., 1984; Kowarski et al., 1985; Somlyo & Himpens, 1990). These gradients increase in response to agents known to release Ca^{2+} from the SR, and to those that increase influx of extracellular Ca^{2+}, and they decrease when influx of extracellular Ca^{2+} is inhibited. In addition to the physiological mechanisms discussed earlier, these gradients could arise from sampling and motion artifacts along the cell edges. However, gradients were present in the great majority of stimulated and unstimulated cells, were present over long periods of observation, were not restricted to cell edges and appeared to be sensitive to physiological stimuli. Artifactual gradients arising from ratioing of image pairs with low signal-to-noise ratios are also unlikely since subplasmalemmal fluorescence gradients were also observed in the respective images before ratioing. Based on these observations we feel strongly that the images obtained in this study represent the two-dimensional projection of a physiological subplasmalemmal $[Ca^{2+}]_i$ gradient. Devine et al. (1972), using electron-microprobe studies, have shown the presence of Ca^{2+} within distinct, yet interconnected components of the SR, the central and the peripheral SR. The peripheral Ca^{2+} storage sites are likely to correspond to the vesicular structures reported in the subplasmalemmal space of a variety of smooth muscle cells and visualized in the current study. Even though additional studies are needed, the structural identity of the Ca^{2+} pool located in one pole of the cell might be the asymmetrically located complex of vesicular structures and mitochondria visualized by electron microscopy in equatorial, longitudinal sections of muscle as shown in Fig. 1, which would correspond to the central pool of Devine's report.

The changes in $[Ca^{2+}]_i$ were oscillatory in nature in every cell examined with an oscillation frequency ranging between 9 and 24 cycles per min. Even though our sampling frequency should fulfill the Nyquist criterion for reliable sampling of these events, aliasing, particularly at higher frequencies, cannot be ruled out. We and others have previously reported oscillatory activity of Ca^{2+}-activated K^+ channels (Benham & Bolton, 1986; Mayer et al., 1989). For example, in whole cell recordings of jejunal myocytes, the frequency of spontaneous tran-

sient outward currents at a holding potential of −40 mV was 13.2 cycles per min, similar to the frequency of $[Ca^{2+}]_i$ oscillations reported here. The frequency decreased with membrane hyperpolarization, but appeared independent of $[Ca^{2+}]_i$ (Benham & Bolton, 1986). A possible physiological importance of the characteristic patterns observed for the $[Ca^{2+}]_i$ signal in this study is suggested by the analogous changes in membrane potential found in myocytes from the longitudinal muscle layer of the mammalian colon (Golenhofen & von Loh, 1970; El-Sharkawy, 1983; Huizinga, Diamant & El-Sharkawy, 1983). In the absence of stimulation, the membrane potential in this tissue remains constant around −70 mV. Agonists produce a characteristic cyclical appearance of potential changes consisting of a slow membrane depolarization with superimposed membrane potential oscillations. The frequency of these oscillations varies between 10 and 35 cycles per min (El-Sharkawy, 1983; Huizinga et al., 1983). These oscillations in turn develop spike potentials at the peak of depolarization. Contractions are associated in a tetanus-like fashion with clusters of oscillations. Similar to their lack of effect on $[Ca^{2+}]_i$ oscillations in this study, agonists do not change the frequency of potential oscillations. In the current study, membrane potential changes were not required for the generation of $[Ca^{2+}]_i$ oscillations.

In excitable cells $[Ca^{2+}]_i$ oscillations can be generated by a membrane oscillator, which results in intermittent influx of extracellular Ca^{2+} through voltage-sensitive Ca^{2+} channels (Schlegel et al., 1987), whereas in nonexcitable cells, intracellular mechanisms are responsible (Berridge & Galione, 1988). Based on the resistance of oscillations to La^{3+} and nifedipine, the origin of the oscillations found in the current study appears to be due more to intracellular recycling across the membrane of the SR and less to plasma membrane entry. However, similar to reports by others (Ambler et al., 1988; Jacob, et al., 1988), we found that refilling of intracellular stores from the extracellular Ca^{2+} pool via voltage-insensitive mechanisms appears to be necessary to maintain oscillations, since lowering extracellular $[Ca^{2+}]$ into the nanomolar range abolished detectable $[Ca^{2+}]_i$ oscillations. In contrast, clamping the membrane potential close to 0 mV in the presence of extracellular $[Ca^{2+}]$ did not affect amplitude or frequency of oscillations. Since the latter protocol will result in transient Ca^{2+} influx (Himpens & Somlyo, 1988) followed by inactivation of voltage-sensitive Ca^{2+} pathways, these findings also suggest that intracellular voltage-insensitive mechanisms are reponsible for the observed $[Ca^{2+}]_i$ oscillations. Thus, the previously reported oscillatory and dihydropyridine-sensitive activation pattern of Ca^{2+}-activated K^+ channels in colonic myocytes in response to substance P (Mayer et al., 1989) seems to be unrelated to the $[Ca^{2+}]_i$ oscillations reported here and may correspond to the generation of spike potentials, superimposed on membrane potential oscillations.

Agonists such as the NK-1 agonist or carbachol and caffeine, which releases Ca^{2+} from the SR, increased amplitude rather than frequency of oscillations. Even though the current results do not rule out the possibility that other cell regulators can modify the frequency of oscillations, they suggest that in myocytes from the longitudinal muscle layer the $[Ca^{2+}]_i$ signal is amplitude rather than frequency modulated. This finding is in contrast to the great majority of reported cell types with cytoplasmic $[Ca^{2+}]_i$ oscillators, in which frequency modulation of the $[Ca^{2+}]_i$ signal has been reported (Berridge & Galione, 1988; Berridge & Irvine, 1989; Cobbold, 1989). However, if the observed $[Ca^{2+}]_i$ oscillations are indeed responsible for slow wave generation in intestinal muscle, the observed lack of frequency modulation is in agreement with the reported constancy of the intestinal slow wave frequency (Cobbold & Rink, 1987).

Different models of cytosolic calcium oscillators have been proposed (Christensen, Caprilli & Lund, 1969; Golenhofen & von Loh, 1970; El-Sharkawy, 1983; Berridge, Cobbold & Cuthbertson, 1988; Meyer & Stryer, 1988; Payne et al., 1988; Gray, 1990). These models fall into the two main categories of receptor-controlled and second messenger-controlled oscillators (Berridge & Galione, 1988). A key concept of the former is the assumption of oscillations in Ins1,4,5P_3 concentrations (Meyer & Stryer, 1988; Cobbold, Cuthbertson & Woods, 1988), whereas in the latter, periodic release of Ca^{2+} in the presence of constant Ins1,4,5P_3 concentrations via feedback loops involving $[Ca^{2+}]_i$ have been proposed (Iino, Kobayashi & Endo, 1988; Payne et al., 1988; Berridge & Irvine, 1989; Gray, 1990). In one type of second messenger-controlled oscillator model, Ins1,4,5P_3 is assumed to release $[Ca^{2+}]_i$ to initiate the transient, but as $[Ca^{2+}]_i$ increases it inhibits further release via negative feedback effect on the release site (Gray, 1990). Our finding that maximal increases in baseline $[Ca^{2+}]_i$ such as seen with high doses of carbachol or K^+ depolarization were associated with a decrease in oscillation amplitude is consistent with such a mechanism.

The current study did not allow us to characterize different encoding strategies depending on the pool of activator Ca^{2+} involved (Cheek, 1989; Kim & Westhead, 1989). For example, K^+ depolarization, receptor-mediated activation and caffeine all showed combinations of changes in baseline $[Ca^{2+}]_i$

and in oscillation amplitude, and an absence of frequency modulation. This pattern of encoding most closely resembles the $[Ca^{2+}]_i$ signalling described in rat parotid acinar cells, a second-messenger controlled $[Ca^{2+}]_i$ oscillator system (Gray, 1990).

Peaks of $[Ca^{2+}]_i$ oscillations did not occur simultaneously in all areas of the cell, and in some cells a clear propagation of the Ca^{2+} signal along the subplasmalemmal space or throughout the cytoplasm in form of a $[Ca^{2+}]_i$ wave was found. Similar spatiotemporal regulation of $[Ca^{2+}]_i$ has been reported in other cell types, including chromaffin cells (Cheek, 1989), astrocytes (Cornell-Bell et al., 1990), hepatocytes (Rooney et al., 1990) and cardiac myocytes (Takamatsu & Wier, 1990). The reported velocities for the $[Ca^{2+}]_i$ waves in these cells ranging from 19 to 100 μm per sec are similar to the values observed in our study. Our failure to detect definitive propagation in all cells studied, may be secondary to the faster propagation velocity in some cells, which would prevent reliable sampling of propagated events with the imaging rate used in this study. In cells with regional structural specializations, such as nonhomogeneous distribution of surface receptors or SR (Cheek, 1989) or functional polarity of the cell (Cheek, 1989; Rooney et al., 1990), the $[Ca^{2+}]_i$ wave originates at a constant pole of the cell. This is similar to our findings in colonic myocytes where propagated $[Ca^{2+}]_i$ gradients originated at the pole of the cell that had the highest $[Ca^{2+}]_i$ during control conditions and following stimulation. The current findings may, therefore, indicate the presence of an intracellular "trigger zone" for the Ca^{2+} signal located within a specialized structure of the central SR and the propagation of the signal along the peripheral SR or throughout the cytoplasm. It remains to be determined if the polarity of Ca^{2+} release in form of a trigger zone arises from asymmetries of intracellular Ca^{2+} compartments (Cheek, 1989) or from an asymmetric distribution of Ca^{2+} release mechanisms. Ca^{2+}-induced Ca^{2+} release mechanisms have been well characterized in cardiac myocytes (Fabiato, 1983) and may be present in colonic smooth muscle (Ilino, 1989). If Ca^{2+}-induced Ca^{2+} release plays a role in propagating the signal, as has been suggested for other cells, an increase of $[Ca^{2+}]_i$ within the trigger zone may set up the necessary gradient for diffusion of Ca^{2+} to the Ca^{2+}-sensitive release sites along the cell membrane, and thence to the cell interior.

The physiological role of propagated $[Ca^{2+}]_i$ gradients is open to question. Given the Ca^{2+}-sensitive conductances present in the plasma membrane of colonic myocytes (Cobbold & Rink, 1987; Mayer et al., 1989), the propagated $[Ca^{2+}]_i$ signal can be expected to result in a corresponding wave of membrane potential and possibly contractile motion. Reported propagation velocities for the slow wave in intact colonic muscle range from 1 to 16 mm per sec (Christensen et al., 1969; Smith, Reed & Sanders, 1987). Given the sampling bias for the lowest range of the spectrum of propagation velocities in the current study, and the temperature difference to the in vivo studies, it is conceivable that the Ca^{2+} waves of individual myocytes provide the basis for slow wave propagation in colonic muscle. If this hypothesis is correct, propagation of Ca^{2+} waves between cells should occur via gap junctions. A paucity of gap junctions in longitudinal intestinal muscle layers has been reported (Gabella, 1989), yet their spatial cellular distribution in this tissue is currently not known. If gap junctions were preferentially located at the cell poles, a propagation of the slow wave and its underlying Ca^{2+} gradient along the longitudinal axis of the gut could be explained.

In conclusion, the findings of the current study are consistent with the hypothesis that the distinct spatio-temporal patterns observed in individual myocytes are the underlying mechanisms for slow wave generation and propagation in colonic smooth muscle.

The authors thank Debbie Anderson for excellent technical assistance with the electron microscopy and Dr. M. Regoli for providing the NK-1 agonist [Sar^9,$Met(O_2)^{11}$]-SP. This work was supported by National Institutes of Health Grants DK 40919 and DK 40675 and Veterans Administration Grant SMI.

References

Alkon, D.L., Rasmussen, H. 1988. A spatial-temporal model of cell activation. *Science* **239:**998–1005

Ambler, S.K., Poenie, M., Tsien, R.Y., Taylor, P. 1988. Agonist-stimulated oscillations and cycling of intracellular free calcium in individual cultured muscle cells. *J. Biol. Chem.* **263:**1952–1959

Benham, C.D., Bolton, T.B. 1986. Spontaneous transient outward currents in single visceral and vascular smooth muscle cells. *J. Physiol.* **381:**385–406

Berridge, M.J. 1988. Inositol trisphosphate-induced membrane potential oscillations in *Xenopus* occytes. *J. Physiol.* **403:**589–599

Berridge, M.J., Cobbold, P.H., Cuthbertson, K.S.R. 1988. Spatial and temporal aspects of cell signalling. *Phil. Trans. R. Soc. London B* **320:**325–343

Berridge, M.J., Galione, A. 1988. Cytosolic calcium oscillators. *FASEB J.* **2:**3074–3082

Berridge, M.J., Irvine, R.F. 1989. Inositol phosphates and cell signalling. *Nature* **341:**197–205

Bitar, K.N., Bradford, P., Putney, J.W., Jr., Makhlouf, G.M. 1986. Cytosolic calcium during contraction of isolated mammalian gastric muscle cells. *Science* **232:**1143–1145

Bond, M., Kitazawa, T., Somlyo, A.P., Somlyo, A.V. 1984. Release and recycling of calcium by the sarcoplasmic reticulum in guinea-pig portal vein smooth muscle. *J. Physiol.* **355:**677–695

Cheek, T.R. 1989. Spatial aspects of calcium signaling. *J. Cell Sci.* **93:**211–216

Christensen, J., Caprilli, R., Lund, G.F. 1969. Electrical slow waves in circular muscle of cat colon. *Am. J. Physiol.* **217:**771–776

Cobbold, P., Cuthbertson, R., Woods, N. 1988. The generation of repetitive free calcium transients in a hormone-stimulated hepatocyte. *In:* Proceedings of the 12th Symposium on Hormones and Cell Regulation, Colloque INSERM. Vol. 165, pp. 135–146. J. Nunez, J.E. Dumont, and P. Carafoli, editors. John Libbey Eurotext, Montrogue, France

Cobbold, P.H. 1989. Oscillatory calcium signals in hormone-stimulated cells. *News Physiol. Sci.* **4:**211–215

Cobbold, P.H., Rink, T.J. 1987. Fluorescence and bioluminescence measurement of cytoplasmic free calcium. *Biochem. J.* **248:**313–328

Cornell-Bell, A.H., Finkbeiner, S.M., Cooper, M.S., Smith, S.J. 1990. Glutamate induces calcium waves in cultured astrocytes: Long-range glial signaling. *Science* **247:**470–473

Devine, C.E., Somlyo, A.V., Somlyo, A.P. 1972. Sarcoplasmic reticulum and excitation-contraction coupling in mammalian smooth muscles. *J. Cell Biol.* **52:** 690–718

El-Sharkawy, T.Y. 1983. Electrical activities of the muscle layers of the canine colon. *J. Physiol.* **342:**67–83

Fabiato, A. 1983. Calcium-induced release of calcium from the cardiac sarcoplasmic reticulum. *Am. J. Physiol.* **245:**C1–C14

Gabella, G. 1989. Structure of intestinal musculature. *In:* Handbook of Physiology. Section 6: The Gastrointestinal System. S.G. Schultz, editor. pp. 103–140. Oxford University Press, New York

Golenhofen, K., von Loh, D. 1970. Elektrophysiologische Untersuchungen zur normalen Spontanaktivitaet der isolierten Taenia Coli des Meerschweinchen. *Pfluegers Arch.* **314:**312–328

Gray, P.T.A. 1990. Oscillations of free cytosolic calcium evoked by cholinergic and catecholaminergic agonists in rat parotid acinar cells. *J. Physiol.* **406:**35–53

Grynkiewicz, G., Poenie, M., Tsien, T.Y. 1985. A new generation of Ca^{2+} indicators with greatly improved fluorescence properties. *J. Biol. Chem.* **260:**3440–3450

Himpens, B., Somlyo, A.P. 1988. Free-calcium and force transients during depolarization and pharmacomechanical coupling in guinea-pig smooth muscle. *J. Physiol.* **395:**507–530

Huizinga, J.D., Diamant, N.E., El-Sharkawy, T.Y. 1983. Electrical basis of contractions in the muscle layers of pig colon. *Am. J. Physiol.* **245:**G482–G492

Ilino, M. 1989. Calcium-induced calcium release mechanism in guinea pig taenia caeci. *J. Gen. Physiol.* **94:**363–383

Ilino, M., Kobayashi, T., Endo, M. 1988. Use of ryanodine for functional removal of the calcium store in smooth muscle cells of the guinea pig. *Biochem. Biophys. Res. Commun.* **152:**417–422

Jacob, R., Merritt, J.E., Hallam, R.J., Rink, T.J. 1988. Repetitive spikes in cytoplasmic calcium evoked by histamine in human endothelial cells. *Nature* **335:**40–45

Kim, K.-T., Westhead, E.W. 1989. Cellular responses to Ca^{2+} from extracellular and intracellular sources are different as shown by simultaneous measurement of cytosolic Ca^{2+} and secretion from bovine chromaffin cells. *Proc. Natl. Acad. Sci. USA* **86:**9881–9885

Kowarski, D., Shuman, H., Somlyo, A.P., Somlyo, A.V. 1985. Calcium release by noradrenaline from central sarcoplasmic reticulum in rabbit pulmonary artery smooth muscle. *J. Physiol.* **366:**153–175

Langton, P.D., Burke, E.P., Sanders, K.M. 1989. Participation of Ca currents in colonic electrical activity. *Am. J. Physiol.* **257:**C451–C460

Martel, A.E., Smith, R.M. 1974. Critical Stability Constants. Vol. 1, Amino Acids. Plenum, New York

Mayer, E.A., Loo, D.D.F., Kodner, A., Reddy, S.N. 1989. Differential modulation of Ca^{2+}-activated K^+ channels by substance P. *Am. J. Physiol.* **257:**G887-G897

Mayer, E.A., Loo, D.D.F., Snape, W.J., Jr., Sachs, G. 1990. The activation of calcium and calcium-activated potassium channels in mammalian colonic smooth muscle by substance P. *J. Physiol.* **420:**47–71

Meyer, T., Stryer, L. 1988. Molecular model for receptor-stimulated calcium spiking. *Proc. Natl. Acad. Sci. USA* **85:**5051–5055

Orchard, C.H., Eisner, D.A., Allen, D.G. 1983. Oscillations of intracellular Ca^{2+} in mammalian cardiac muscle. *Nature* **304:**735–738

O'Sullivan, A.J., Cheek, T.R., Moreton, R.B., Berridge, M.J., Burgoyne, R.D. 1989. Localization and heterogeneity of agonist-induced changes in cytosolic calcium concentration in single bovine adrenal chromaffin cells. *EMBO J.* **8:**401–411

Payne, R., Walz, B., Levy, S., Fein, A. 1988. The localization of calcium release by inositol trisphosphate in *Limulus* photoreceptor and its control by negative feedback. *Phil. Trans. R. Soc. London B* **320:**359–379

Rooney, T.A., Sass, E.J., Thomas, A.P. 1990. Agonist-induced cytosolic calcium oscillations originate from a specific locus in single hepatocytes. *J. Biol. Chem.* **265:**10792–10796

Schlegel, W., Winiger, B.P., Mollard, P., Vacher, P., Wuarin, F., Zahnd, G.R., Wollheim, C.B., Dufy, B. 1987. Oscillations of cytosolic Ca^{2+} in pituitary cells due to action potential. *Nature* **329:**719–721

Smith, T.K., Reed, J.B., Sanders, K.M. 1987. Interaction of two electrical pacemakers in muscularis of canine proximal colon. *Am. J. Physiol.* **252:**C290–C299

Somlyo, A.P., Himpens, B. 1990. Cell calcium and its regulation in smooth muscle. *FASEB J.* **3:**2266–2276

Takamatsu, T., Wier, W.G. 1990. Calcium waves in mammalian heart: Quantification or origin, waveform, and velocity. *FASEB J.* **4:**1519–1525

Takuwa, Y., Takuwa, N., Rasmussen, H. 1990. Measurement of cytoplasmic free Ca^{2+} concentration in bovine tracheal smooth muscle using aquorin. *Am. J. Physiol.* **253:**C817–C827

Tsunoda, Y., Stuenkel, E.L., Williams, J.A. 1990. Oscillatory mode of calcium signaling in rat pancreatic acinar cells. *Am. J. Physiol.* **258:**C147–C155

Williams, D.A., Becker, P.L., Fay, F.S. 1987. Regional changes in calcium underlying contraction of single smooth muscle cells. *Science* **235:**1644–1648

Williams, D.A., Fogarty, K.E., Tsien, R.Y., Fay, F.S. 1985. Calcium gradients in single smooth muscle cells revealed by the digital imaging microscope using Fura-2. *Nature* **318:**558–561

Woods, N.M., Cuthbertson, K.S.R., Cobbold, P.H. 1986. Repetitive transient rises in cytoplasmic free calcium in hormone-stimulated hepatocytes. *Nature* **319:**600–719

Woods, N.M., Cuthbertson, K.S.R., Cobbold, P.H. 1987. Agonist-induced oscillations in cytoplasmic free calcium concentration in single rat hepatocytes. *Cell Calcium* **8:**79–100

Received 29 October 1991; revised 5 June 1991